S.Z. Imamaliyeva[*1], I.F. Mekhdiyeva[1], Y.I. Jafarov[2], M.B. Babanly[1]

[1]Institute of Catalysis and Inorganic Chemistry named after acad. M. Nagiyev,
Azerbaijan National Academy of Sciences, Baku, Azerbaijan;
[2]Baku State University, Azerbaijan
([*]Corresponding author's e-mail: samira9597a@gmail.com)

Thermodynamic study of the thallium-thulium tellurides by EMF method

In this study the phase equilibria in the $Tl_2Te–Tl_2Te_3–TlTmTe_2$ compositions area of the Tl–Tm–Te ternary system were studied by powder X-ray diffraction (PXRD) analysis. Based on PXRD data, the solid-phase equilibria diagram was plotted. The thermodynamic functions of the Tl_9TmTe_6 and $TlTmTe_2$ ternary compounds were calculated by the electromotive forces method. The electrochemical cells of the following type $(−)$ TmTe (s.) | glycerol + KCl + $TmCl_3$ | (Tm in alloys of Tl–Tm–Te system) (s.) $(+)$ were assembled and their EMF were measured in the 300-450 K temperature range. Based on obtained EMF data for the $Tl_2Te_3–TlTe–TlTmTe_2$ and $TlTe–TlTmTe_2–Tl_9TmTe_6$ three-phase regions, the relative partial thermodynamic functions of TmTe in alloys were calculated. The combination of these functions with the partial molar functions of thulium in TmTe allowed calculating the corresponding partial functions of thulium in the above phase regions. The potential-forming reactions responsible for the indicated partial molar values were obtained based on constructed solid-phase equilibria diagram. Using indicated potential-forming reactions, for the first time, the standard thermodynamic functions of formation and standard entropies of the Tl_9TmTe_6 and $TlTmTe_2$ compounds were calculated.

Keywords: Tl–Tm–Te system, Tl_9TmTe_6, $TlTmTe_2$, powder X-ray diffraction analysis, solid-phase equilibria diagram, method of electromotive forces, concentration cells, thermodynamic functions.

Introduction

The presence of a wide range of functional properties (thermoelectric, optical, electronic) in chalcogenides of heavy elements makes them promising functional materials in numerous fields of modern technology, such as electronics, optoelectronics industry, photovoltaic and photo-detection applications, fiber-optical communication, etc. [1–6]. Moreover, the discovery of a topological insulators (TI) shown that these compounds also exhibit the properties of TI and can be used in spintronics and quantum computers, medicine, security systems [7, 8].

The introduction of heavy metal atoms as well as d- and f-elements into the crystal lattice of these compounds can lead to an improvement in their thermoelectric properties [9], and also give them additional functionality, for example, magnetic properties, as well as the properties of TI [10–13].

It is known that telluride Tl_5Te_3 exhibits thermoelectric properties [14]. Due to the peculiarities of the crystal lattice it has many ternary analogs of the types Tl_9AX_6 and Tl_4BX_3 (A-Sb, Bi, In, Au, rare-earth elements; B-Sn, Pb, Mo, Cu, rare-earth elements; X-Se, Te) [15–22], also possessing several functional properties, namely optical [23, 24], thermoelectric [25–27], magnetic [28, 29], as well as topological insulators properties [30, 31]. In recent years in order to improve thermoelectric performance intensive work has been carried out to study solid solutions and doped phases based on these compounds [32–34].

Another class of thallium chalcogenides with the common formula $TlCX_2$ (C – Sb, Bi, In, Ag, rare-earth elements) also possess many functional properties [10, 35–40].

For design and optimization of the synthesis and the growth of the single crystal conditions besides the phase diagram, accurate data of the thermodynamic functions are required [43–46]. Usually, the method of differential scanning calorimetry is used to determine the thermal effects of phase transformations and the heat capacity [47, 48]. At the same time, the method of electromotive forces (EMF) has found wide application in practice due to the simplicity of measurements and their high accuracy. EMF measurements are often used to investigate the partial and integral thermodynamic functions of formation. In practice, the several modifications of the EMF method are used. In this case, liquid electrolytes [49–51], solid electrolytes [52, 53], as well as ionic liquids can serve as an electrolyte [54, 55].

However, despite potential interest we did not find in the literature data on the thermodynamic properties of Tl_9LnTe_6 and $TlLnX_2$ compounds. Considering the above, we have undertaken a comprehensive study of solid-phase equilibria and thermodynamic properties of the Tl–Gd–Te and Tl–Er–Te systems [41, 42].

In this experimental study, we present the results of the investigation of the solid-phase relations in the Tl_2Te-Tl_2Te_3-$TlTmTe_2$ system and the thermodynamic properties of the Tl_9TmTe_6 и $TlTmTe_2$ ternary compounds by EMF method.

Experimental

Synthesis

The initial compounds and intermediate samples from the Tl_2Te_3–$TlTe$–$TlTmTe_2$ and $TlTe$–$TlTmTe_2$–Tl_9TmTe_6 three-phase regions were synthesized from high-purity thallium (granules, 99.999 %), thulium (ingots, 99.9%), tellurium (ingots 99.999 %), and telluride Tl_2Te in evacuated quartz ampoules. After alloying at 1000 K, non-homogenized intermediate samples were powdered, mixed, compressed into a tablet, and annealed further at 700 K for 1000 h.

The congruently melting Tl_2Te was synthesized by fusing thallium and tellurium in vacuumed ($\sim 10^{-2}$ Pa) quartz ampoule at 750 K followed by slow cooling.

The refractory compound TmTe was synthesized by ceramic method at 1000 K followed by annealing at 900 K for 1000 h.

Methodology

Studies were carried out by powder X-ray phase diffraction analysis (Bruker D8 diffractometer with $CuK\alpha_1$ radiation) and electromotive forces (EMF) method.

For the rational planning of thermodynamic experiments, we first studied the solid-phase equilibria of the Tl–Tm–Te system in the Tl_2Te–Tl_2Te_3–$TlTmTe_2$ compositions area (Fig. 1).
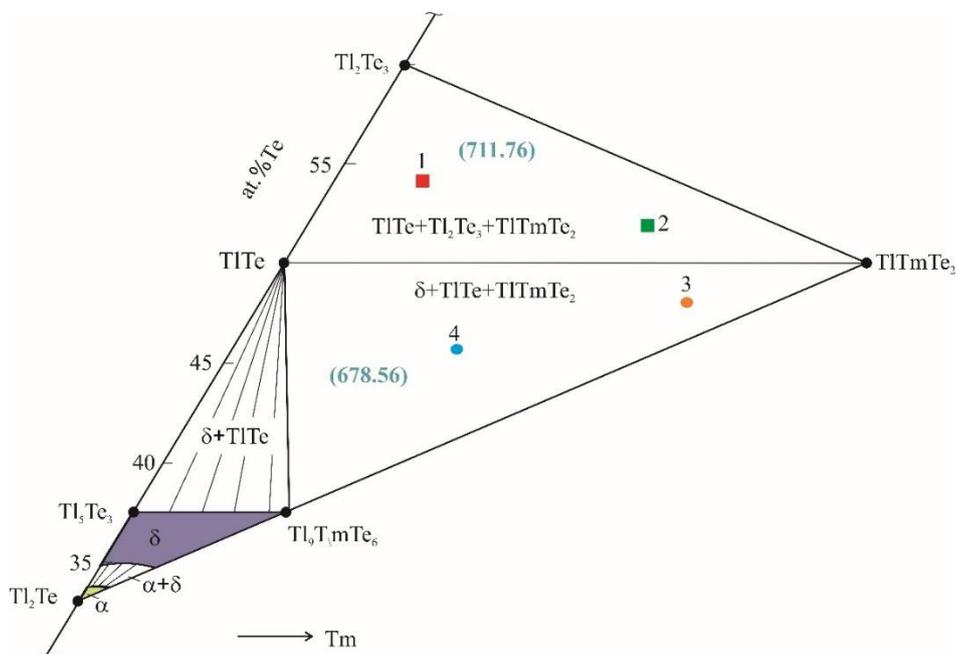

Figure 1. The solid-phase equilibria diagram of the Tl_2Te–Tl_2Te_3–$TlTmTe_2$ subsystem.
1–4 — alloy compositions used for XRD and EMF measurements;
the numbers in brackets are the EMF values (mV) of the cells type (1) in the three-phase regions

The data on phase relations in the Tl_2Te–Tl_5Te_3–Tl_9TmTe_6 composition area were taken from the previous study [56]. The formation of a wide area of solid solutions with the Tl_5Te_3 structure (δ-phase) was found for this system. Also it was established that δ-phase is tie-lined to TlTe (Fig. 1) [57]. As a result, a two-phase region δ+TlTe is formed on the phase diagram. Solid-phase equilibria diagram of the Tl_2Te_3–Tl_2Te–$TlTmTe_2$ system also reflects the presence of three-phase regions Tl_2Te_3–$TlTe$–$TlTmTe_2$ and $TlTe$–$TlTmTe_2$–Tl_9TmTe_6 (Fig.1). Their existence is confirmed based on powder diffraction patterns of selected alloys (Fig. 2, samples 1, 4).
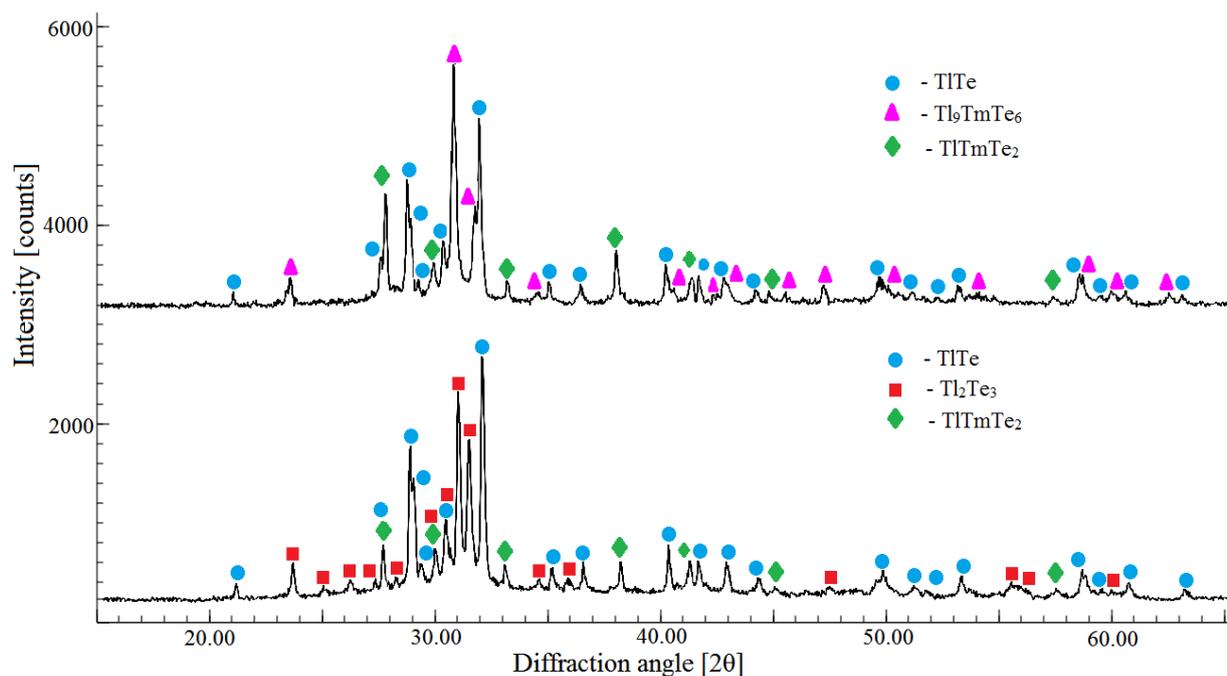
Figure 2. The powder X-ray diffractogramms of the alloys from Tl_2Te_3–$TlTe$–$TlTmTe_2$
and $TlTe$–$TlTmTe_2$–Tl_9TmTe_6 compositions areas

Thus, EMF measurements in the indicated three-phase regions can be used for calculations of the thermodynamic functions of the Tl_9TmTe_6 and $TlTmTe_2$ ternary compounds.

The assembled electrochemical cell with a liquid electrolyte can be presented schematically as

$$(-) \ TmTe \ (s.) \ | \ glycerol + KCl + TmCl_3 \ | \ (Tm \ in \ alloys) \ (s.) \ (+). \qquad (1)$$
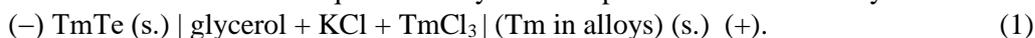
In cells (1) a glycerol solution of KCl with addition of $TmCl_3$ (0.1 %) was used as the electrolyte. It is necessary to pay special attention to the salts (KCl и $TmCl_3$) and glycerol. They must be free from moisture and oxygen. Therefore glycerol was dehydrated and degassed before use by pumping at a temperature of ~450 K. Anhydrous KCl and $TmCl_3$ were used. The electrolyte was stored in a sealed ampoule and used as required. Upon the introduction of the electrolyte in a cell, contact with air was minimal.

TmTe with a negligible (0.1 at.%) tellurium excess was used as the left (negative) electrode. Our previous studies [41, 42] showed that using metallic lanthanide as the left electrode resulted in high EMF values. Right (positive) electrodes in the cells of type (1) were equilibrium alloys from Tl_2Te_3–$TlTe$–$TlTmTe_2$ and $TlTe$–$TlTmTe_2$–Tl_9TmTe_6 three-phase regions. The synthesis of the alloys - right electrodes is described above. The methods for preparing electrodes and assembling an electrochemical cell are detailed described in [54, 55]. To control the reproducibility of the EMF results and their compliance with the phase diagram, 2 electrode-alloys with different compositions from each three-phase region were prepared.

The electrochemical cell described [54, 55] was assembled, evacuated, filled with argon, and placed in a cylindrical electric furnace. All contacts and current leads of the cell were kept at the same temperature. The first equilibrium EMF values were obtained after keeping the concentration cell at ~350 K for 60 h, followed by every 3–4 hours after the establishment of a certain temperature. The EMF data were considered equilibrium if they did not differ from each other upon repeated measurements at a given temperature by more than 0.2 mV, regardless of the direction of the temperature change. Within the experiment the EMF of each sample was measured 3 times at two constant temperatures. For example, for an alloy from the Tl_2Te–Tl_5Te_3–Tl_9TmTe_6 phase region at 350.8 K, EMF values were: 683.13, 683.19, 683.224. Table 1 presents the averaged value of 683.18.

Keithley 2100 6 1/2 digital multimeter was used for EMF measurements. Most measurements were carried out when heating and cooling the cell in steps no more than 10°. The chromel-alumel thermocouples and a mercury thermometer (an accuracy of ±0.5 K) were used for measurements of the temperature of the electrochemical cell.

The EMF measurements were conducted in 300–450 K temperature interval. The upper limit of the temperature interval of the EMF measurements was chosen so that the phase composition remained unchanged within the experiment. The mass measurement and X-ray diffraction analysis of electrodes before and after EMF measurements were used to control the reversibility of electrochemical cells and reproducibility of results. The mass and composition of the electrodes remained constant in the time of the experiment.

Results and Discussion

The obtained experimental data, i.e., pairs of temperature and EMF values are listed in Table 1.

T a b l e 1

**Experimentally determined data for temperature and EMF of the Tl_2Te_3–TlTe–$TlTmTe_2$
and TlTe–$TlTmTe_2$–Tl_9TmTe_6 phase regions in the Tl–Tm–Te system**

T, K	E, mV	
	TlTe–$TlTmTe_2$–Tl_9TmTe_6	Tl_2Te_3–TlTe–$TlTmTe_2$
301.2	680.24	712.85
306.7	679.15	711.34
312.7	681.02	712.45
318.3	679.84	714.64
323.3	681.68	715.12
328.2	681.82	713.13
334.2	682.08	715.65
340.1	680.62	713.94
345.5	684.68	714.02
350.8	683.18	718.12
357.7	684.24	714.94
362.2	683.21	719.08
366.4	684.86	719.66
371.5	684.86	716.06
377.9	688.84	720.07
382.9	687.68	717.98
387.4	687.44	716.46
392.3	685.02	719.66
395.3	688.44	719.22
402.1	688.68	722.12
407.5	690.96	718.78
412.3	688.12	719.83
416.7	688.93	722.55
421.3	687.87	721.88
425.7	693.46	722.74
431.1	692.21	722.66
437.2	693.34	722.02
442.7	692.66	724.33
446.2	693.85	724.12
449.2	693.99	725.97

The EMF measurements data of the electrochemical cell of type (1) were in full agreement with the diagram of solid-phase equilibria of the Tl_2Te–Tl_2Te_3–$TlTmTe_2$ system (Fig. 1). At a certain temperature the EMF value in the three-phase regions Tl_2Te_3–TlTe–$TlTmTe_2$ and TlTe–$TlTmTe_2$–Tl_9TmTe_6 were constant and changed during the transition from one phase to another.

The temperature dependences on EMF for all alloys of the Tl-Tm-Te system were linear (Fig.3). Also, the measurements results showed that, in addition to reproducibility, the numerical values of the EMF increase in the radial directions from Tm vertex of the Tl–Tm–Te concentration triangle, which is in agreement with the well-known thermodynamic principle [47, 48].
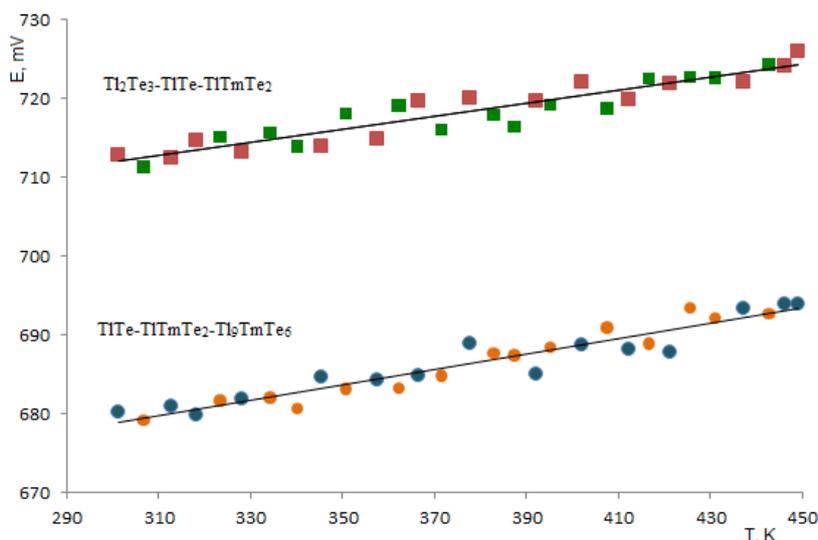
Figure 3. Temperature dependencies of EMF for alloys of the Tl_2Te_3–TlTe–$TlTmTe_2$
and TlTe–$TlTmTe_2$–Tl_9TmTe_6 phase areas of the Tl-Tm-Te system.
Alloys of different composition for each three-phase area are shown in different colors

Alloy designations are the same as in Figure 1.

Therefore, the data obtained were processed by the least-squares method, and temperature dependences of EMF were represented by the linear equation of type

$$E = a + bT \pm t \left[\frac{\delta_E^2}{n} + \delta_b^2 (T - \overline{T})^2 \right]^{1/2}. \tag{2}$$

In equation (2) a and b are coefficients, n is the number of pairs of values E and T; $\overline{T}$ is average temperature in K, t is Student's test, and δ_E^2 and δ_b^2 are the variances of individual EMF values and the constant b. With the number of experimental points $n = 30$, and the confidence level equal to 95 %, the Student's test is $t \le 2$. Table 2 lists the equations obtained.

The partial molar functions of thulium telluride in the alloys at 298 K (Table 3) were calculated using the following thermodynamic relations:

$$\Delta \overline{G}_{TmTe} = -zFE; \tag{3}$$

$$\Delta \overline{S}_{TmTe} = zF \left(\frac{\partial E}{\partial T} \right)_P = zFb; \tag{4}$$

$$\Delta \overline{H}_{TmTe} = -zF \left[E - T \left(\frac{\partial E}{\partial T} \right)_P \right] = -zFa. \tag{5}$$

In the equations (3)–(5), z is the charge of the potential-forming cation Tm^{3+}, F is the Faraday constant, a and b are the constants in relation (2).

Table 2

Temperature dependencies of the EMF for the cells of the type (1) in the 300–450 K temperature interval

№	Phase area	E, mV $= a + bT \pm 2[\delta_E^2 / n + \delta_b^2 (T - \overline{T})]^{1/2}$
1	Tl_2Te_3 + TlTe + $TlTmTe_2$	$687.07 + 0.0828T \pm 2 \left[\dfrac{2.1}{30} + 3.5 \cdot 10^{-5} (T - 378.2) \right]^{1/2}$
2	TlTe + Tl_9TmTe_6 + $TlTmTe_2$	$649.22 + 0.0984T \pm 2 \left[\dfrac{1.9}{30} + 3.1 \cdot 10^{-5} (T - 378.2) \right]^{1/2}$

Relative partial molar functions of thulium monotelluride in the alloys of the Tl-Tm-Te system at T = 298 K

Phase area	$-\overline{\Delta G}_{TmTe}$	$-\overline{\Delta H}_{TmTe}$	$\overline{\Delta S}_{TmTe}$
	kJ·mol^{-1}		J·mol^{-1}·K^{-1}
Tl$_2$Te$_3$ + TlTe + TlTmTe$_2$	206.02±0.31	198.88±1.30	23.97±3.40
TlTe + Tl$_9$TmTe$_6$ + TlTmTe$_2$	196.42±0.30	187.92±1.23	28.48±3.24

These values represent the difference of the corresponding partial molar functions of thulium for the left and right electrodes of the cells of type (1). For example, for alloys from Tl$_2$Te$_3$ + TlTe + TlTmTe$_2$ three-phase area

$$\Delta \overline{G}_{TmTe}(\text{in alloys}) = \Delta \overline{G}_{Tm}\ (\text{in alloy}) - \Delta \overline{G}_{Tm}(\text{in TmTe}),$$

then

$$\Delta \overline{G}_{Tm}\ (\text{in alloy}) = \Delta \overline{G}_{TmTe}\ (\text{in alloy}) + \Delta \overline{G}_{Tm}(\text{in TmTe}). \qquad (6)$$

Therefore, the calculation of the partial thermodynamic functions of thulium in the above three-phase regions was carried out by summation of the data in Table 3 with the corresponding partial molar functions Tm in TmTe [58]: $\Delta \overline{G}_{Tm} = -261.31\pm0.22$ кJ·mol^{-1}, $\Delta \overline{H}_{Tm} = -267.62\pm0.92$ кJ·mol^{-1}, $\Delta \overline{S}_{Tm} = -21.16\pm2.42$ J·mol^{-1}·K^{-1}. The obtained results are given in Table 4.

Relative partial molar functions of thulium in the alloys of the Tl–Tm–Te system at T = 298 K

Phase area	$-\overline{\Delta G}_{Tm}$	$-\overline{\Delta H}_{Tm}$	$\overline{\Delta S}_{Tm}$
	kJ·mol^{-1}		J·mol^{-1}·K^{-1}
Tl$_2$Te$_3$ + TlTe + TlTmTe$_2$	467.33±0.53	466.50±2.22	2.78±5.82
TlTe + Tl$_9$TmTe$_6$ + TlTmTe$_2$	457.73±0.52	455.54±2.15	7.35±5.66

The standard integral thermodynamic functions of the TlTmTe$_2$ and Tl$_9$TmTe$_6$ compounds were calculated by the method of potential-forming reactions. According to the solid-phase equilibria diagram (Fig. 1), the values of the partial molar functions of thulium in the Tl$_2$Te$_3$–TlTe–TlTmTe$_2$ and TlTe–TlTmTe$_2$–Tl$_9$TmTe$_6$ three-phase areas are thermodynamic functions of the potential formation reactions

$$Tm + Tl_2Te_3 = TlTe + TlTmTe_2 \qquad (7)$$
$$Tm + 3TlTe = 0.25Tl_9TmTe_6 + 0.75TlTmTe_2 \qquad (8)$$
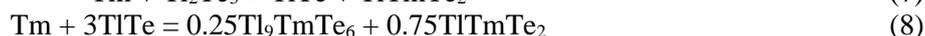
According to relations (7) and (8), the standard thermodynamic functions of the formation of ternary compounds TlTmTe$_2$ and Tl$_9$TmTe$_6$ can be calculated from the relations

$$\Delta_f Z^0(\text{TlTmTe}_2) = \overline{\Delta Z}_{Tm} + \Delta_f Z^0(\text{Tl}_2\text{Te}_3) - \Delta_f Z^0(\text{TlTe}), \qquad (9)$$

$$\Delta_f Z^0(\text{Tl}_9\text{TmTe}_6) = 4\overline{\Delta Z}_{Tm} + 12\Delta_f Z^0(\text{TlTe}) - 3\Delta_f Z^0(\text{TlTmTe}_2), \qquad (10)$$

(Z≡G, H), while the standard entropy by using relations

$$S^0(\text{TlTmTe}_2) = \overline{\Delta S}_{Tm} + S^0(\text{Tm}) + S^0(\text{Tl}_2\text{Te}_3) - S^0(\text{TlTe}), \qquad (11)$$

$$S^0(\text{Tl}_9\text{TmTe}_6) = 4\overline{\Delta S}_{Tm} + 4S^0(\text{Tm}) + 12S^0(\text{TlTe}) - 3S^0(\text{TlTmTe}_2). \qquad (12)$$

Using relations (9)–(12) in calculations, beside own experimental data (Table 4), the value of the standard entropy Tm (71.014±0.209 kJ·mol^{-1}) [59] as well as thermodynamic data for TlTe and Tl$_2$Te$_3$ (Table 5), determined by using the EMF method [60] and included in the database [59] were used.

When calculating relations (10) and (12), in addition to the partial molar functions of thulium in the three-phase region TlTe+Tl$_9$TmTe$_6$+TlTmTe$_2$ we used the standard integral thermodynamic functions of the TlTmTe$_2$ compound determined in this work (Table 5).

Standard integral thermodynamic functions of thallium-thulium tellurides at T= 298 K

Compound	$-\Delta_f G^0(298K)$	$-\Delta_f H^0(298K)$	$S^0(298K)$
	kJ·mol^{-1}		J·mol^{-1}·K^{-1}
TlTe [60]	44.5±0.4	44.9±0.5	115.9±1.5
Tl$_2$Te$_3$ [60]	90.8±0.8	90.0±1.0	279.7±3.3
TlTmTe$_2$	513.6±1.7	511.6±3.7	240.6±10.8
Tl$_9$TmTe$_6$	824.1±12.0	826.2±25.7	965.0±74.0

During the calculations of the partial thermodynamic functions of thulium (Table 4) and integral thermodynamic functions of ternary compounds (Table 5), the inaccuracies were determined by the uncertainty propagation method. The relatively high errors in the values of the enthalpy of formation and entropy can be explained by the fact that, in contrast to the usual potential-forming reactions with one final product, there are 2 final products in reactions (7) and (8). Therefore, when calculating the thermodynamic functions of TlTmTe$_2$ and Tl$_9$TmTe$_6$ compounds according to relations (9)–(12), the thermodynamic functions of some compounds are subtracted from the general balance, while their errors are summed up.

Conclusion

In this paper we presented a set of experimental data on solid-phase relations in the Tl–Tm–Te ternary system in the Tl$_2$Te–Tl$_2$Te$_3$–TlTmTe$_2$ composition interval and thermodynamic functions of the TlTmTe$_2$ and Tl$_9$TmTe$_6$ compounds obtained by the powder XRD and EMF methods. The relative partial thermodynamic functions of TmTe and Tm in alloys were obtained based on the EMF measurements. The potential-forming reactions responsible for the above partial molar quantities were determined based on constructed solid-phase equilibria diagram, and the standard thermodynamic functions of formation and standard entropies of the TlTmTe$_2$ and Tl$_9$TmTe$_6$ compounds were calculated for the first time.

Acknowledgment

On behalf of all authors, the corresponding author states that there is no conflict of interest.

References

1   Liu, X., Lee, S., Furdyna, J.K., Luo, T., & Zhang, Y.H. (2019). *Chalcogenide. From 3D to 2D and Beyond*. Elsevier.

2   Alonso-Vante, N. (2018). *Chalcogenide Materials for Energy Conversion: Pathways to Oxygen and Hydrogen Reactions*. Publisher Springer International Publishing AG

3   Scheer, R., & Hans-Werner, S. (2011). *Chalcogenide Photovoltaics: Physics, Technologies, and Thin Film Devices*. Wiley-VCH.

4   Woodrow, Ph. (2018). *Chalcogenides: Advances in Research and Applications*. Nova.

5   Ahluwalia, G.K. (2016). *Applications of Chalcogenides: S, Se, and Te*. Springer.

6   Berger, L.I. (1997). *Semiconductor Materials*. CRC Press, Boca Raton, FL.

7   Holtgrewe, K., Mahatha, S.K., Sheverdyaeva, P.M., Moras P., Flammini, R., & Colonna, S., et al. (2020). Topologization of β-antimonene on Bi$_2$Se$_3$ via proximity effects. *Scientific Reports, 10*, 14619-14612. https://doi.org/10.1038/s41598-020-71624-4

8   Flammini, R., Colonna, S., Hogan, C., Mahatha, S., Papagno, M., & Barla, A., et al. (2018). Evidence of β-antimonene at the Sb/Bi$_2$Se$_3$ interface. *Nanotechnology, 29(6)*, 065704-8. https://doi.org/ 10.1088/1361-6528/aaa2c4

9   Ioffe, A.F. (1957). Semiconductor Thermoelements and Thermoelectric Cooling. *Infosearch Limited*, London.

10   Filnov, S.O., Klimovskikh, I.I, Estyunin, D.A., Fedorov, A., Voroshnin, V., & Koroleva, A.V., et al. (2020). Probe-dependent Dirac-point gap in the gadolinium-doped thallium-based topological insulator TlBi$_{0.9}$Gd$_{0.1}$Se$_2$. *Physical Review B, 102*, 085149-7. https://doi.org/10.1103/PhysRevB.102.085149

11   Usanmaz, D., Pinku, N., Toher, C., Plata, J.J., Friedrich, R., & Fornari, M., et al. (2018). Spinodal Superlattices of Topological Insulators. *Chemical Materials, 30(7)*, 2331–2340. https://doi.org/10.1021/acs.chemmater.7b05299

12   Shi, Y., Mashmoushi, N., Wegner, W., Jafarzadeh, P., Sepahi, Z., Assoud, A., & Kleinke, H. (2019). Ultralow thermal conductivity of Tl$_4$Ag$_{18}$Te$_{11}$. *Journal of Material Chemistry C, 7*, 8029–8036. DOI: 10.1039/c9tc02029b

13 Ong, M., Hammouri, M., & Jishi, R.A. (2018). Ab Initio Study of Optoelectronic and Magnetic Properties of Ternary Chromium Chalcogenides. *Advances in Materials Science and Engineering,* 1–6. DOI: 10.1155/2018/3762451

14   Matsumoto, H., Kurosaki, K., Muta, H., & Yamanaka, Sh. (2009). Thermoelectric Properties of the Thallium-Tellurium Binary Compounds. *Materials Transactions*, *50(7)*, 1582–1585. https://doi.org/10.2320/matertrans.E-M2009803

15 Wacker, K. (1991). Die kristalstrukturen von Tl_9SbSe_6 und Tl_9SbTe_6. *Z. Kristallogr. Supple*, *3*, 281.

16 Doert, T., & Böttcher, P. (1994). Crystal structure of bismuthnonathalliumhexatelluride $BiTl_9Te_6$. *Z. Kristallogr., 209*, 95. https://doi.org/10.1524/zkri.1994.209.1.95.15

17 Bradtmöller, S., & Böttcher, P. (1993). Darstellung und kristallostructur von $SnTl_4Te_3$ und $PbTl_4Te_3$. *Zeitschrift für anorganische und allgemeine Chemie*, *619,* 1155–1160. https://doi.org/10.1002/zaac.19936190702

18 Imamaliyeva, S.Z., Babanly, D.M., Tagiev, D.B., & Babanly, M.B. (2018). Physicochemical Aspects of Development of Multicomponent Chalcogenide Phases Having the Tl_5Te_3 Structure. *A Review Russian Journal of Inorganic Chemistry, 63,* 1703–1724. https://doi.org/10.1134/S0036023618130041

19 Imamaliyeva, S.Z. (2020). Tl_4GdTe_3 and Tl_4DyTe_3 — Novel Structural Tl_5Te_3 Analogues. *Physics and chemistry of solid State*, *21(3),* 492–495. DOI: 10.15330/pcss.21.3.492-495

20 Imamaliyeva, S.Z. (2020). New thallium tellurides with rare earth elements. *Condensed Matter and Interphases*. 4, 460-465. https://doi.org/10.15330/pcss.21.3.492-495

21 Bradtmöller, S., & Böttcher, P. (1994). Crystal structure of copper tetra thallium tritelluride $CuTl_4Te_3$. *Zeitschrift für Kristallographie*, *209(1),* 97. https://doi.org/10.1524/zkri.1994.209.1.97

22 Bradtmöller, S., & Böttcher, P. (1994). Crystal structure of molybdenum tetra thallium tritelluride, $MoTl_4Te_3$. *Zeitschrift für Kristallographie*, *209(1),* 75. https://doi.org/10.1524/zkri.1994.209.1.75

23 Piasecki, M., Brik, M.G., & Barchiy, I.E. (2017). Band structure, electronic and optical features of Tl_4SnX_3 (X= S, Te) ternary compounds for optoelectronic applications. *Journal of Alloys and Compounds*, *710,* 600–607. https://doi.org/10.1016/j.jallcom.2017.03.280

24 Barchij, I.E., Sabov, M., & El-Naggar, A.M. (2016). Tl_4SnS_3, Tl_4SnSe_3 and Tl_4SnTe_3 crystals as novel IR induced optoelectronic materials. *Journal of Materials Science: Mater Electron*, *27*, 3901–3905. https://doi.org/10.1007/s10854-015-4240-4

25 Kurosaki, K., Uneda, H., Muta, H., & Yamanaka, S. (2004). Thermoelectric properties of thallium antimony telluride. *Journal of Alloys and Compounds*, *376,* 43–48, https://doi.org/10.1016/j.jallcom.2004.01.018

26 Guo, Q., & Kleinke, H. (2015). Thermoelectric properties of hot-pressed (Ln = La, Ce, Pr, Nd, Sm, Gd, Tb) and $Tl_{10-x}La_xTe_6$ (0,90<x<1,05). *Journal of Alloys and Compounds, 630*, 37–42. https://doi.org/10.1016/j.jallcom.2015.01.025

27 Heinke, F., Eisenburger, L., & Schlegel, R. (2017). The Influence of Nanoscale Heterostructures on the Thermoelectric Properties of Bi-substituted Tl_5Te_3. *Zeitschrift für anorganische und allgemeine Chemie, 643*, 447–454. https://doi.org/10.1002/zaac.201600449

28 Bangarigadu-Sanasy, S., Sankar, C.R., Dube, P.A., Greedan, J.E., & Kleinke, H. (2014). Magnetic properties of Tl_9LnTe_6, Ln = Ce, Pr, Tb and Sm. *Journal of Alloys and Compounds, 589*, 389–392. https://doi.org/10.1016/j.jallcom.2013.11.229

29 Isaeva, A., Schönemann, R., & Doert, T. (2020). Syntheses, crystal structure and magnetic properties of Tl_9RETe_6 (RE = Ce, Sm, Gd*). Crystals — Open Access Journal, 10(4),* 1–11. https://doi.org/10.3390/cryst10040277

30 Arpino, K.E., Wasser, B.D., & McQueen, T.M. (2015). Superconducting Dome and Crossover to an Insulating State in $[Tl_4]Tl_{1-x}Sn_xTe_3$. *APL Materials*, *3(4)*, 041507-8. https://doi.org/10.1063/1.4913392

31 Niu, C., Dai, Y., Huang, B., Bihlmayer, G., Mokrousov, Y., Wortmann, D., & Blügel, S. (2014). Natural three-dimensional topological insulators in Tl_4PbTe_3 and Tl_4SnTe_3. *Frühjahrstagung der Deutschen Physikalischen Gesellschaft*, 01899.

32 Waqas, M.Kh., Altaf, U.R., Tufail, M., Ibrar, M., Wiqar, H. Sh., Waqar, A. S., & Gul, B. (2020). Toward controlled thermoelectric properties of Pb and Sb co-doped nanostructured Thallium Telluride for energy applications. *Materials Research Express 7*, 105010-13. https://doi.org/10.1088/2053-1591/abbb54

33 Guo, Q., Assoud, A., & Kleinke, H. (2014). Improved Bulk Materials with Thermoelectric Figure-of-Merit Greater than 1: $Tl_{10-x}Sn_xTe_6$ and $Tl_{10-x}Pb_xTe_6$. *Materials Science. Advanced Energy Materials, 4(14)*, 1400348-8. https://doi.org/10.1002/aenm.201400348

34   Kuropatwa, B.A., Guo, Q., Assoud, A., & Kleinke, H. (2014). Optimization of the Telluride $Tl_{10-x-y}Sn_xBi_yTe_6$ for Thermoelectric Properties. *Zeitschrift für anorganische und allgemeine Chemie, 640*, 774–780. https://doi.org/10.1002/zaac.201200284

35 Singh, B., Sharma, A., Lin, H., Hasan, M. Z., Prasad, R., & Bansil, A. (2012). Topological electronic structure and Weyl semimetal in the $TlBiSe_2$ class of semiconductors. *Physical Review B, 86*, 115208-7. DOI: 10.1103/PhysRevB.86.115208

36 Pielmeier, F., Landolt, G., Slomski, B., Mu, S., Berwanger, J., & Eich, A., et al. (2015). Response of the topological surface state to surface disorder in $TlBiSe_2$. *New Journal of Physics, 17*, 023067-8. https://doi.org/10.1088/1367-2630/17/2/023067

37 Ding, G., He, J., Cheng, Z., Wang, X., & Li, S. (2018). Low lattice thermal conductivity and promising thermoelectric figure of merit of Zintl type $TlInTe_2$. *Journal of Materials Chemistry*, *6*, 13269–13274. https://doi.org/10.1039/C8TC03492C

38   Shi, Y., Guo, Q., Cheng, X., Jafarzadeh, P., Macario, L. R., Menezes, L., & Kleinke, H. (2019). Thermoelectric properties of $TlSbTe_2$ doped with In and Yb. *Journal of Alloys and Compounds, 795*, 1–7. https://doi.org/10.1016/j.jallcom.2019.04.294

39 Sankar, C.R., Bangarigadu-Sanasy, S., & Kleinke, H. (2012). Thermoelectric properties of $TlGdQ_2$ (Q=Se, Te) and Tl_9GdTe_6. *Journal of Electronic Materials*, *41*, 1662–1666. https://doi.org/10.1007/s11664-011-1846-z

40 Duczmal, M. (2003). *Structure, wlasciwosci magnetzcyne i pole krzstalicyne w potrojnzch chalkogenkach lantonowcow i talu $TlLnX_2$ (X=S, Se lub Te)*. Monografie, Politechniki Wroclawskiej.

41 Imamalieva, S.Z., Babanly, D.M., Gasanly, T.M., Tagiev, D.B., & Babanly, M.B. (2018). Thermodynamic Properties of Tl_9GdTe_6 and $TlGdTe_2$. *Russian Journal of Physical Chemistry A, 92 (11)*, 2111–2117. https://doi.org/10.1134/S0036024418110158

42 Imamaliyeva, S.Z., Mekhdiyeva, I. F., Babanly, D.M., Zlomanov, V.P., Tagiyev, D.B., & Babanly, M.B. (2020). Solid-Phase Equilibria in the $Tl_2Te–Tl_2Te_3–TlErTe_2$ System and the Thermodynamic Properties of the Tl_9ErTe_6 and $TlErTe_2$ Compounds, *Russian Journal of Inorganic Chemistry*. 65(*11*), 1762–1769. https://doi.org/10.1134/S0036023620110066

43 Babanly, M.B., Mashadiyeva, L.F., Babanly, D.M., Imamaliyeva, S.Z., Taghiyev, D.B., & Yusibov, Y.A. (2019). Some aspects of complex investigation of the phase equilibria and thermodynamic properties of the ternary chalcogenid systems by the EMF method. *Russian Journal of Inorganic Chemistry*, *64 (13),* 1649–1671. https://doi.org/10.1134/S0036023619130035

44 Imamaliyeva, S.Z. (2018). Phase diagrams in the development of thallium-REE tellurides with Tl_5Te_3 structure and multicomponent phases based on them. *Condensed Matter and Interphases, 20*(*3*), 332–347. https://doi.org/10.17308/kcmf.2018.20/570

45 Matsushita, T., & Mukai, K. (2018). *Chemical Thermodynamics in Materials Science: From Basics to Practical Applications*, Springer, 257

46 Morachevsky, A.G., Voronin, G.F., Geyderich, V.A., & Kutsenok, I.B. (2003). *Electrochemical methods of investigation in thermodynamics of metal systems*. Akademkniga Publishing, 334.

47 Jain, A., & Kandan, R. (2018). Determination of the thermodynamic stability of europium boride (EuB_6). *Thermal Analysis and Calorimetry*, 132(1), 275–283. https://doi.org/10.1007/s10973-017-6876-1

48 Dahshan, A., Alharbi, S.R., Aly, K.A., & Saddeek, Y. (2020). Thermal, mechanical, electrical and thermoelectric properties of Bi–As–Se glasses. *Thermal Analysis and Calorimetry*, *140*(*1*), 125–131. https://doi.org/10.1007/s10973-019-08810-8

49 Vassiliev, V.P., Lysenko, V., & Bros, J. (2019). Thermodynamic study of the Ag-In-Sn system by the EMF method. *Journal of Alloys and Compounds, 790,* 370–376. https://doi.org/10.1016/J.JALLCOM.2019.03.016

50 Imamaliyeva, S.Z., Mehdiyeva, I.F., Taghiyev, D.B., & Babanly, M.B. (2020). Thermodynamic investigations of the erbium tellurides by EMF method. *Physics and Chemistry of Solid State, 21(2),* 312–318. https://doi.org/10.15330/pcss.21.2.312-318

51 Imamaliyeva, S.Z., Babanly, D.M., Zlomanov, V.P., Taghiyev, D.B., & Babanly, M.B. (2020). Thermodynamic properties of terbium tellurides. *Condensed Matter and Interphases, 4,* 453–459. https://doi.org/10.17308/kcmf.2020.22/3116

52 Moroz, M., Tesfaye, F., Demchenko, P., Prokhorenko, M., & Lindberg, D. (2018). Phase equilibria and thermodynamics of selected compounds in the Ag–Fe–Sn–S system. *Journal of Electronic Materials, 47 (9),* 5433-5442. https://doi.org/10.1007/s11664-018-6430-3

53 Moroz M., Tesfaye F., Demchenko P., Prokhorenko M., Kogut Y., & Pereviznyk O., et al. (2020). Solid-state electrochemical synthesis and thermodynamic properties of selected compounds in the Ag–Fe–Pb–Se system. *Solid State Science,* 107, 106344-9. https://doi.org/10.1016/j.solidstatesciences.2020.106344

54 Aliev, Z.S. Musayeva, S.S., Imamaliyeva, S.Z., & Babanly, M.B. (2018). Thermodynamic study of antimony chalcoiodides by EMF method with an ionic liquid. *Journal of Thermal Analysis and Calorimetry, 133(2),* 1115–1120. https://doi.org/10.1007/s10973-017-6812-4

55 Imamaliyeva, S.Z., Musayeva, S.S., Babanly, D.M., Jafarov, Y.I., Tagiyev, D.B., & Babanly, M.B. (2019). Determination of the thermodynamic functions of bismuth chalcoiodides by EMF method with morpholinium formate as electrolyte. *Thermochimica Acta,* 679, 178319-7. https://doi.org/10.1016/j.tca.2019.178319

56 Imamaliyeva, S.Z., Mekhdiyeva, I.F., Amiraslanov, I.R., & Babanlı, M.B. (2017). Phase equilibria in the Tl_2Te–Tl_5Te_3–Tl_9TmTe_6 section of the Tl-Tm-Te system. Phase equilibria and diffusion, 38(5), 764–770. https://doi.org/10.1007/s11669-017-0564-5

57 Mekhdiyeva, I.F. (2021). Phase equilibria in the $TlTe$–Tl_9TmTe_6 system. *Azerbaijan Chemical Journal, 1*, 32–37.

58 Imamaliyeva, S.Z., Mekhdiyeva, I.F., Gasymov, V.A., Babanli, D.M., Taghiyev, D.B., & Babanli, M.B. (2021). Solid-phase equilibria and thermodynamic properties of phases of the Tm-Te system. *Russian Journal of Physical Chemistry. C, 95(5)*, 926–932.

59 Thermal constants of substances: Database. Version 2, 2006. http://www.chem.msu.ru/cgi-bin/tkv.pl?show=welcome.html/welcome.html

60 Vasilev, V.P., Nikolskaya, A.V., Gerasimov, Ya.I., Kuznetsov, A.F. (1969). Thermodynamic investigation of thallium telluride by the electromotive force method. *Neorg. Mater. 4(7)*, 1040–1047.

С.З. Имамалиева, И.Ф. Мехдиева, Я.И. Джафаров, М.Б. Бабанлы

Талий-тулий теллуридтерін ЭҚК әдісімен термодинамикалық зерттеу

Мақалада Tl_2Te–Tl_2Te_3–$TlTmTe_2$ композициялар диапазонындағы фазалық тепе-теңдікті Tl–Tm–Te үштік жүйесінің ұнтақты рентгендік дифракциясы арқылы зерттеу нәтижелері келтірілген. XRD деректері негізінде қатты фазалық тепе-теңдік диаграммасы құрылды. Tl_9TmTe_6 және $TlTmTe_2$ үштік қосылыстарының термодинамикалық қасиеттері электр қозғаушы күштер әдісімен анықталды. (–) TmTe (қатты) типіндегі электрохимиялық ұяшықтар жиналды (қатты.) | глицерин + KCl + $TmCl_3$ | (Tl Tl–Tm–Te жүйесінің қорытпаларында) (қатты) (+) және олардың ЭҚК температурасы 300–450 К температурасында өлшенді. Алынған ЭҚК деректері негізінде үш фазалы аймақтар үшін Tl_2Te_3–$TlTe$–$TlTmTe_2$ және $TlTe$–$TlTmTe_2$–Tl_9TmTe_6, қорытпалардағы TmTe салыстырмалы ішінара термодинамикалық функциялары анықталды. Бұл функцияларды тулийдің TmTe ішінара молярлық функцияларымен біріктіре отырып, жоғарыда аталған фазалық аймақтардағы тулийдің сәйкес ішінара функциялары есептеледі. Қатты фазалық тепе-теңдік сызбасын қолдана отырып, көрсетілген ішінара молярлық шамаларға жауап беретін потенциал түзуші реакцияларды пайдаланып, Tl_9TmTe_6 және $TlTmTe_2$ қосылыстарының стандартты термодинамикалық функциялары және стандартты энтропиялары есептелді.

Кілт сөздер: Tl–Tm–Te жүйесі, Tl_9TmTe_6, $TlTmTe_2$, функционалды материалдар, рентгендікфазалық талдау, қаттыфазалық тепе-теңдік диаграммасы, электр қозғаушы күштер әдісі, термодинамикалық функциялар.

С.З. Имамалиева, И.Ф. Мехдиева, Я.И. Джафаров, М.Б. Бабанлы

Термодинамическое исследование теллуридов талия-тулия методом ЭДС

В статье представлены результаты исследования фазовых равновесий в области составов Tl_2Te–Tl_2Te_3–$TlTmTe_2$ тройной системы Tl–Tm–Te методом порошковой рентгеновской дифракции. На основании данных РФА построена диаграмма твердофазных равновесий. Термодинамические свойства тройных соединений Tl_9TmTe_6 и $TlTmTe_2$ определены методом электродвижущих сил. Были собраны электрохимические ячейки типа (−) TmTe (тв.) | глицерин + KCl + $TmCl_3$ | (Tm в сплавах системы Tl-Tm-Te) (тв.) (+) и измерены их ЭДС в интервале температур 300–450 К. На основании полученных данных ЭДС для трехфазных областей Tl_2Te_3–$TlTe$–$TlTmTe_2$ и $TlTe$–$TlTmTe_2$–Tl_9TmTe_6 определены относительные парциальные термодинамические функции TmTe в сплавах. Комбинируя эти функции с парциальными молярными функциями тулия в TmTe, вычислены соответствующие парциальные функции тулия в указанных выше фазовых областях. Используя диаграмму твердофазных равновесий, составлены потенциалобразующие реакции, отвечающие за указанные парциальные молярные величины. С использованием составленных потенциалобразующих реакций впервые рассчитаны стандартные термодинамические функции образования и стандартные энтропии соединений Tl_9TmTe_6 и $TlTmTe_2$.

Ключевые слова: система Tl–Tm–Te, Tl_9TmTe_6, $TlTmTe_2$, функциональные материалы, рентгенофазовый анализ, диаграмма твердофазных равновесий, метод электродвижущих сил, термодинамические функции.

Information about authors:

Imamaliyeva, Samira Zakir — PhD on chemistry, Associate professor, Senior researcher, Institute of Catalysis and Inorganic Chemistry named after acad. M. Nagiyev, Azerbaijan National Academy of Sciences, 113, H. Javid ave., Baku, AZ-1143, Azerbaijan; e-mail: samira9597a@gmail.com; https://orcid.org/0000-0001-8193-2122

Mekhdiyeva, İlaha Firudin — PhD student, researcher, Institute of Catalysis and Inorganic Chemistry named after acad. M. Nagiyev, Azerbaijan National Academy of Sciences, 113, H. Javid ave., Baku, AZ-1143, Azerbaijan; e-mail: mehdiyeva.ilahe2@gmail.com; https://orcid.org/0000-0002-1106-0207

Jafarov, Yasin Isa — Doctor on chemistry, Associate professor, Baku State University, 23, Z, Khalilov str., Baku, Az-1048, Azerbaijan; e-mail: yasin.cafarov@hotmail.com; https://orcid.org/0000-0002-6597-2252

Babanly, Mahammad Baba – corresponding member of ANAS, doctor on chemistry, deputy-director, Institute of Catalysis and Inorganic Chemistry named after acad. M. Nagiyev, Azerbaijan National Academy of Sciences, 113, H. Javid ave., Baku, AZ-1143, Azerbaijan; e-mail: babanlymb@gmail.com; https://orcid.org/0000-0001-5962-3710